LETTERS

Supercurrent reversal in quantum dots

Jorden A. van Dam[1], Yuli V. Nazarov[1], Erik P. A. M. Bakkers[2], Silvano De Franceschi[1,3] & Leo P. Kouwenhoven[1]

When two superconductors are electrically connected by a weak link—such as a tunnel barrier—a zero-resistance supercurrent can flow[1,2]. This supercurrent is carried by Cooper pairs of electrons with a combined charge of twice the elementary charge, *e*. The 2*e* charge quantum is clearly visible in the height of voltage steps in Josephson junctions under microwave irradiation, and in the magnetic flux periodicity of *h*/2*e* (where *h* is Planck's constant) in superconducting quantum interference devices[2]. Here we study supercurrents through a quantum dot created in a semiconductor nanowire by local electrostatic gating. Owing to strong Coulomb interaction, electrons only tunnel one-by-one through the discrete energy levels of the quantum dot. This nevertheless can yield a supercurrent when subsequent tunnel events are coherent[3–7]. These quantum coherent tunnelling processes can result in either a positive or a negative supercurrent, that is, in a normal or a π-junction[8–10], respectively. We demonstrate that the supercurrent reverses sign by adding a single electron spin to the quantum dot. When excited states of the quantum dot are involved in transport, the supercurrent sign also depends on the character of the orbital wavefunctions.

The electronic properties of quantum dots can be probed by attaching source and drain electrodes, allowing charge carriers to tunnel from the dot to both electrodes. If the electrodes are superconducting, transport is strongly affected and largely depends on the transparency of the electrical connection between the electrodes and the quantum dot. A number of experiments have focused on various phenomena in the Coulomb blockade regime but no supercurrents through quantum dots were observed, mostly due to the lack of a controllable tunnel coupling with the electrodes[11–14]. Strong coupling and negligible Coulomb interactions were recently obtained in carbon nanotube quantum dots demonstrating resonant tunnelling of Cooper pairs through a single quantum state[15]. In the regime of strong Coulomb interactions, the simultaneous occupation of the quantum dot with two electrons is unfavourable. Nevertheless, a supercurrent can flow owing to the subsequent (but coherent) transport of correlated electrons. This can give rise to a sign change of the Cooper pair singlet (that is, from $(|\uparrow\downarrow\rangle - |\downarrow\uparrow\rangle)/\sqrt{2}$ to $e^{i\pi}(|\uparrow\downarrow\rangle - |\downarrow\uparrow\rangle)/\sqrt{2}$, where $\uparrow$ and $\downarrow$ represent the two eigenstates of the z component of the spin). Therefore, the typical Josephson relation between the supercurrent, I_s, and the macroscopic phase difference between the superconductors, φ, usually given by $I_s = I_c \sin(\varphi)$, changes to $I_s = I_c \sin(\varphi + \pi) = -I_c \sin(\varphi)$ (ref. 5; I_c is the critical current). Other mechanisms of Cooper pair transport resulting in negative supercurrents have been studied using high-transition-temperature superconductors[8], ferromagnets[9], and non-equilibrium mesoscopic normal metals[10].

We use indium arsenide (InAs) nanowires as semiconductor weak links[16] in combination with local gate electrodes in order to obtain quantum dots with a tunable coupling to superconducting leads. The monocrystalline n-type InAs nanowires are grown by a catalytic process based on the vapour–liquid–solid growth method[17–20]. After growth, the wires are transferred to an oxidized silicon substrate. Previously developed nanofabrication techniques are used to define highly transparent aluminium-based superconducting contacts[16]. Pairs of nearby nanowires are contacted in parallel, forming a superconducting loop with two nanowire junctions (Fig. 1a). In a second lithographic step, we define local gate electrodes. One of the nanowires (top nanowire in Fig. 1a) is crossed by two gates, labelled L and R, in order to define a quantum dot (also see Fig. 1b). The bottom nanowire is crossed by one gate, labelled REF, and will be used as a reference junction with a tunable Josephson coupling. We have studied two similar devices in detail. Here we present the results for one of them. Similar data from the second device and further details on device fabrication are given as Supplementary Information.

Below the superconducting transition temperature of the aluminium-based contacts ($T_c \approx 1.1$ K), the two nanowires form superconducting weak links owing to the proximity effect[16], thereby realizing a superconducting quantum interference device (SQUID)[2]. The critical current of the SQUID, I_c, as a function of magnetic flux, Φ, shows oscillations with a period of 66 μT. This is consistent with the addition of a flux quantum, $\Phi_0 = h/2e$, to the effective SQUID area of 30 μm^2 (Fig. 1c, blue trace, temperature $T = 30$ mK). The maximum (minimum) critical current corresponds to the sum (difference) of the critical currents of the two nanowire junctions. Unlike in other SQUIDs, the critical currents of the individual junctions can be tuned by applying voltages to the respective gates. This is demonstrated by a measurement of the SQUID oscillations for different voltages applied to REF. When $V_{REF} = -0.64$ V (Fig. 1c, green trace), the amplitude of the SQUID oscillations is reduced owing to the partial local depletion of the nanowire. By further reducing the gate voltage to $V_{REF} = -0.80$ V, the reference junction is pinched off, resulting in the disappearance of the interference signal. We thus have a unique electrical control over the SQUID operation.

A quantum dot is formed in the top nanowire by applying negative voltages simultaneously to gates L and R. The local depletion creates two tunnel barriers, which define a single quantum dot in the nanowire section between the gates (see Fig. 2a inset), giving rise to discrete energy levels and Coulomb blockade. To show this, we pinch off the reference junction ($V_{REF} = -0.80$ V) and apply a small magnetic field in order to suppress superconductivity. Figure 1d shows a colour plot of absolute current through the quantum dot, $|I|$, as a function of bias voltage, V, and gate voltages, $V_L = V_R$. Coulomb blockade ($|I| = 0$) occurs within continuous diamond-shaped regions, as is typically observed in transport through single quantum dots[21]. Outside these regions, $|I|$ increases in steps (lines parallel to the diamond edges) denoting the onset of single-electron tunnelling via discrete excited states. From the separation between these lines, we estimate for this regime a characteristic level spacing of ~1 meV. The sharpness of the diamond edges and the excitation lines denote a weak tunnel coupling between the quantum dot and the source and drain leads. We can increase the coupling by reducing the negative

[1]Kavli Institute of Nanoscience, Delft University of Technology, PO Box 5046, 2600 GA, Delft, The Netherlands. [2]Philips Research Laboratories, High Tech Campus 4, 5656 AE Eindhoven, The Netherlands. [3]Laboratorio Nazionale TASC INFM-CNR, Area Science Park, S.S. 14, Km. 163.5, I-34012 Trieste, Italy.

voltages applied to L and R (see Fig. 1e). This results in blurred diamond edges (dotted lines) and the appearance of inelastic co-tunnelling features inside the diamonds. This tunable coupling is particularly important for reaching the narrow transport regime where charging effects dominate but, at the same time, the critical current is large enough to be measurable.

Switching to the superconducting state but with the reference junction still pinched off, two peaks in dI/dV develop around $V \approx \pm 200\,\mu V = \pm 2\Delta^*/e$ (Fig. 2b). $2\Delta^*$ is the superconducting gap induced in the nanowire by the proximity effect (Fig. 2a inset). These features are due to second-order co-tunnelling, and the peak shape reflects the singularities in the quasiparticle density of states at the gap edges. In spite of the Coulomb blockade effect, we observe a finite supercurrent, $I_{c,qd}$, through the nanowire quantum dot. We exploit the SQUID geometry to determine the critical value and the sign of this supercurrent in a current-biased measurement[22]. When an integer number of flux quanta are applied through the SQUID area, the critical current of the SQUID corresponds to the sum of the critical currents of the two junctions[2], that is, $I_c = I_{c,qd} + I_{c,REF}$. We set $I_{c,REF} = 320$ pA, and extract the V_L-dependence of $I_{c,qd}$ directly from the measurement of I_c (Fig. 2a). We find $I_{c,qd} < 0$ for two charge states of the quantum dot, denoted by a yellow diamond and a yellow square in Fig. 2b. The negative supercurrent of the quantum dot junction is confirmed by the $\Phi_0/2$ shift between the SQUID oscillations for $I_{c,qd} < 0$ (Fig. 2c, red trace) and those for $I_{c,qd} > 0$ (blue trace). A colour plot of $I_c(V_L, \Phi)$ in Fig. 2d shows the transitions between positive and negative supercurrents around the charge state denoted by the yellow square.

Negative supercurrents have been predicted for superconductors coupled by a magnetic impurity or a single-level interacting quantum dot[3–5,7]. In these systems resonant tunnelling of Cooper pairs is prohibited owing to Coulomb blockade. Nevertheless, Cooper pairs can be transported via fourth-order co-tunnelling events. Three examples of such events are shown in Fig. 3. The top and bottom diagrams are the initial and final states, respectively, and the

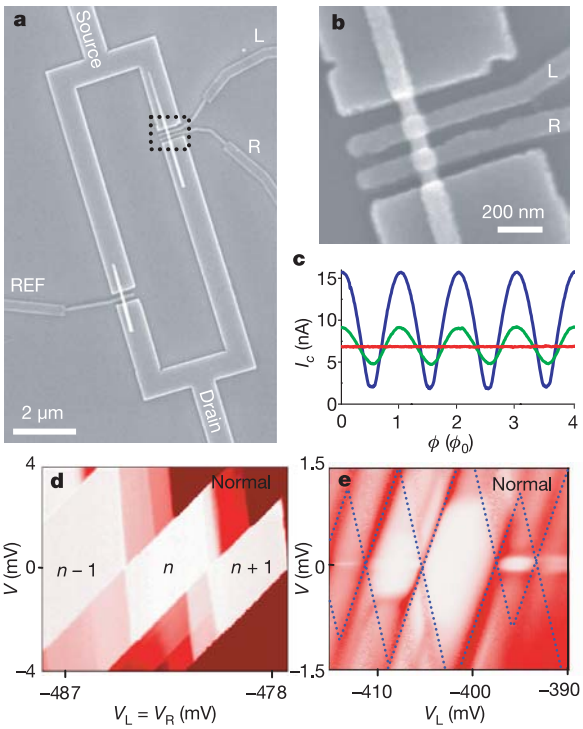

Figure 1 | Sample layout and device characterization. **a**, Scanning electron micrograph of the InAs nanowire SQUID. Two nanowires (diameter ~60 nm) are incorporated in a superconducting loop (100 nm Al on 10 nm Ti). Aluminium top-gates (L and R) with a spacing of ~65 nm are used to define a quantum dot in the top nanowire. A third gate (REF) is used to control the reference junction. **b**, High-resolution image of the top nanowire shown boxed in **a**. **c**, Critical current of the SQUID, I_c, versus magnetic flux, Φ (in units of the flux quantum, Φ_0), for different voltages applied to the reference gate ($V_{REF} = 0$ V (blue trace), -0.64 V (green), and -0.80 V (red)), demonstrating full electrical control over the amplitude of the SQUID oscillations. **d**, Colour plot of absolute current through the dot, $|I|$, (increasing from white (0 pA) to red (5 pA)) versus source–drain bias voltage, V, and $V_L = V_R$ in the normal state. The Coulomb diamonds are well defined owing to the weak tunnel coupling between quantum dot and leads. **e**, Differential conductance, dI/dV (increasing from white (0.1 μS) to red (40 μS)), as a function of V and V_L ($V_R = -0.40$ V). The stronger dot–lead coupling results in blurred diamond edges (indicated by dotted lines) and horizontal features inside the diamonds due to inelastic co-tunnelling. Data in **d** and **e** are taken at $T = 30$ mK, and in a small magnetic field to drive the superconducting contacts into the normal state.

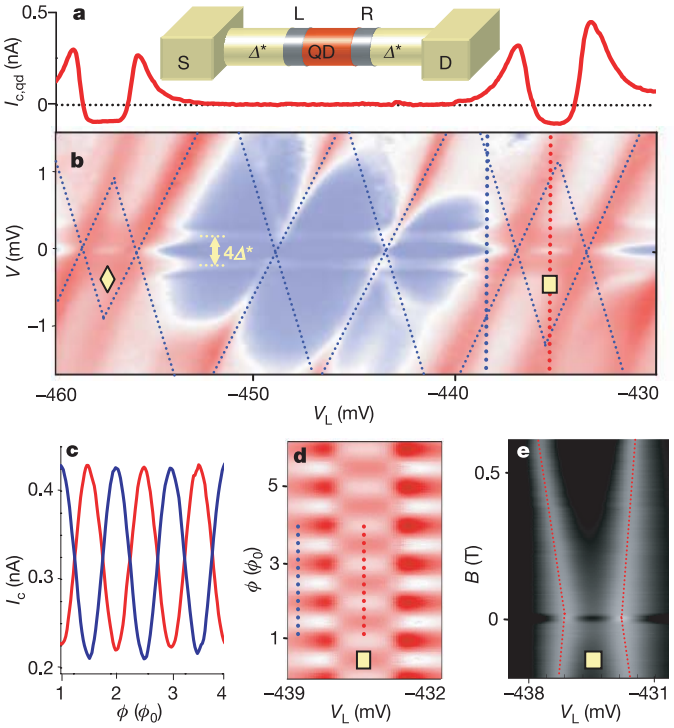

Figure 2 | Supercurrent reversal in an interacting quantum dot. **a**, Plot of the critical current of the quantum dot, $I_{c,qd}$, as a function of gate voltage, V_L, for the same gate voltage region as in **b**. QD, quantum dot; S, source; D, drain. A negative supercurrent is observed for two charge states. Inset, diagram of the quantum dot in the nanowire. **b**, Colour scale plot of differential conductance, $dI/dV(V, V_L)$, in the superconducting state (dI/dV increases from blue, through white, to red; $V_{REF} = -0.8$ V). The two peaks in dI/dV at $V \approx \pm 200\,\mu V$ are due to quasiparticle co-tunnelling, and their spacing ($4\Delta^*$ as indicated) provides a direct measurement of the induced superconducting gap in the nanowire. Yellow symbols (diamond and square) indicate two charge states that exhibit negative supercurrent. Blue dotted lines indicate the diamond edges. **c**, Two $I_c(\Phi)$ curves taken at gate voltages indicated by the vertical red and blue dotted lines in **b**, demonstrating the shift by $\Phi_0/2$ between the conventional (blue) and the π-regime (red). **d**, Critical current of the SQUID, I_c, in colour-scale as a function of Φ and V_L. Yellow square: the interference signal is shifted by half a flux quantum compared to adjacent Coulomb diamonds, indicating the π-shift in the Josephson relation. Red and blue dotted lines correspond to red and blue traces in **c**. Individual $I_c(\Phi)$ curves can be fitted very well with a sine-function within the measurement accuracy. **e**, Grey-scale plot of linear conductance, G (increasing from black to white), as a function of magnetic field, B, and V_L. Yellow square: the Coulomb peak spacing in this charge state increases with increasing field owing to the Zeeman effect, indicating that the number of electrons is odd. All measurements are taken at $T = 30$ mK. Note that the measurements in **a**, **c** and **d** are current-biased and in **b** and **e** voltage-biased.

diagrams in between show one of the three intermediate virtual states. Owing to Coulomb blockade, a sequence of intermediate states involves an energy cost comparable to the charging energy, E_c (for $\Delta^* \ll E_c$). Nevertheless, when the tunnel rate is on the order of E_c/h, a Cooper pair can be transported by higher-order co-tunnelling events[23]. In principle, there are 24 possible sequences of 4 tunnel events. However, in a single-level quantum dot only a small number of sequences are allowed. Figure 3a illustrates the transfer of a Cooper pair through a quantum dot with a single spin-degenerate level occupied by one electron (with spin up, $|\uparrow\rangle$). The sequence of four tunnel processes, indicated by the numbers, is necessarily permuted compared to ordinary transport of Cooper pairs. The remarkable result is that the spin-ordering of the Cooper pair is reversed, that is, the Cooper pair on the right is created in the order $|\uparrow\rangle, |\downarrow\rangle$ while the pair on the left is annihilated in the order $|\downarrow\rangle, |\uparrow\rangle$. This spin-reversal results in a sign-change of the Cooper pair singlet state (for example, from $(|\uparrow\downarrow\rangle - |\downarrow\uparrow\rangle)/\sqrt{2}$ to $e^{i\pi}(|\uparrow\downarrow\rangle - |\downarrow\uparrow\rangle)/\sqrt{2}$), leading to a π-shift in the Josephson relation and a negative supercurrent. However, if an extra electron is added to the quantum dot, the sequence of tunnel events discussed above is prohibited, owing to the Pauli exclusion principle. Now other sequences of tunnel events are allowed, which result in a normal, positive supercurrent[7] (Fig. 3b). Therefore, in a single-level quantum dot a negative (positive) supercurrent is expected for an odd (even) number of electrons.

We can discriminate between odd and even numbers of electrons in Fig. 2b by measuring the linear conductance, G, as a function of gate voltage and magnetic field, B (Fig. 2e). We observe that the Coulomb peak spacing for the two charge states denoted by the yellow square and diamond increases owing to the Zeeman effect, demonstrating that for these charge states the occupation number, n, is odd[21] (only data for the state denoted by a yellow square is shown, $|g\text{-factor}| \approx 15$, similar to previous results for similar systems[24]). These observations are consistent with the model described above.

However, for the charge state around $V_L = -447$ mV with an odd number of electrons, we observe a very small, but positive critical current ($I_c \approx 10$ pA). Moreover, in a different gate voltage range, shown in Fig. 4a, supercurrent reversal is also observed for charge states with an even number of electrons. We argue that these observations originate from co-tunnelling via multiple energy levels of the quantum dot. The multi-level nature of the quantum dot for the gate range studied in Fig. 4a emerges from the measurement of differential conductance in the normal state (Fig. 1e). Here several peaks parallel to the diamond edges are observed, which correspond to transport through excited states of the quantum dot. In this gate voltage range the level spacing, δ, is of the order of E_c. Therefore, these excited states can take part in co-tunnelling events and the simple model of a single-level quantum dot is no longer appropriate. As a result, all 24 sequences of tunnel events are allowed for both odd and even numbers of electrons. Therefore, a negative supercurrent due to permutation of tunnel events is possible for all values of n (refs 7, 25).

Additionally, in the multi-level regime, properties of the wavefunctions of the quantum dot become important. To illustrate this, we consider the co-tunnelling event in Fig. 3c in which two different energy levels are involved in a dot with an even number of electrons. Because the two electrons take a different path, they can acquire a different phase. The opposite parity of the wavefunctions results in a

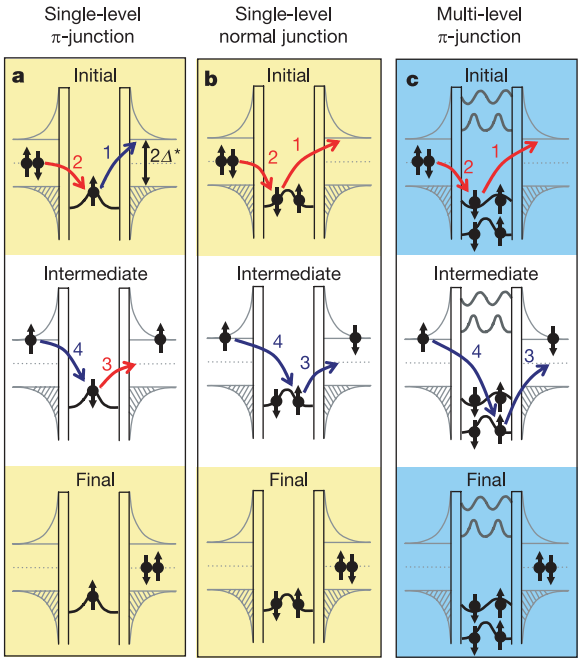

Figure 3 | Energy diagrams illustrating Cooper pair transport through a quantum dot due to fourth-order co-tunnelling. Top and bottom panels represent initial and final states, respectively. The intermediate panels show one of the three virtual intermediate states. Numbers indicate the sequence of tunnel events. Red (blue) corresponds to the tunnelling of a spin-down (spin-up) electron. **a**, Transport occurs through a single spin-degenerate level filled with one electron. During this event the spin-ordering of the Cooper pair is reversed. This results in a negative contribution to the supercurrent (see also diagrams in ref. 5). **b**, Transport through one spin-degenerate level filled with two electrons. The spin-ordering of the Cooper pair cannot be reversed, resulting always in a positive supercurrent. **c**, Co-tunnelling event involving two energy levels with wavefunctions of opposite parity. This results in a negative contribution to the supercurrent[7].

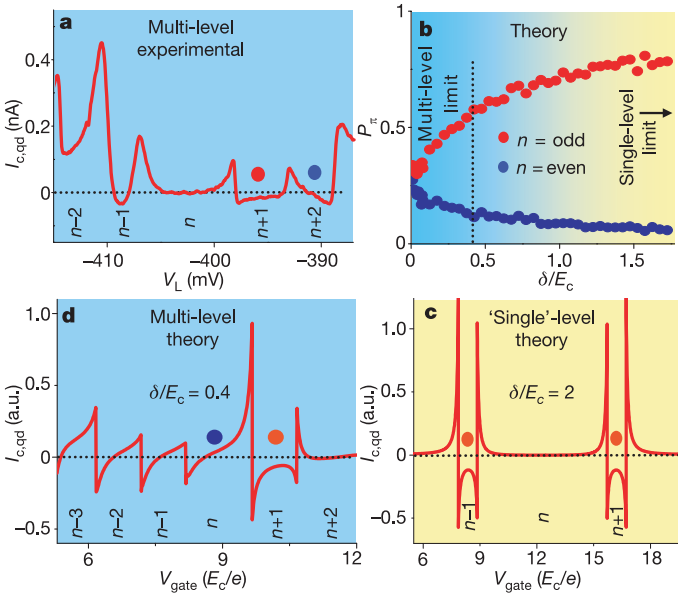

Figure 4 | Experimental results and numerical simulations for a multi-level quantum dot. Panels are ordered clockwise. **a**, Measured critical current of the quantum dot, $I_{c,qd}$, as a function of V_L, showing supercurrent reversal for even and odd numbers of electrons (indicated by a blue and red dot, respectively; $V_R = -0.4$ V). **b**, Calculated probability of π-behaviour, P_π, for odd (red) and even (blue) numbers of electrons as a function of δ/E_c. Strength and sign of tunnel couplings are randomly varied. For $\delta/E_c \gg 1$, the limiting case of a single-level quantum dot is reached, resulting in π-behaviour for odd numbers and conventional behaviour for even numbers of electrons. In the multi-level limit ($\delta/E_c \ll 1$), we obtain $P_\pi \approx 0.3$ for both even and odd numbers of electrons. **c**, Calculated critical current, $I_{c,qd}$, as a function of gate voltage, V_{gate}, for $\delta/E_c = 2$. For odd numbers of electrons (red dots), the critical current is typically negative, similar to the measurement shown in Fig. 2a. **d**, $I_{c,qd}(V_{gate})$ for $\delta/E_c = 0.4$. Negative supercurrents are found for both odd (red dot) and even numbers of electrons (blue dot), as in the experimental data shown in **a**.

phase difference of π and therefore this event contributes to a negative supercurrent[7] (see Supplementary Information). So, for a multi-level dot two effects can result in supercurrent reversal: permutation of tunnel events and an opposite parity of wavefunctions. When co-tunnelling events with a negative contribution dominate, the junction will exhibit a negative supercurrent. We note that the presence of the Kondo effect[26,27] can result in a positive supercurrent where otherwise a negative supercurrent would be expected[28,29]. We have not found any evidence for the Kondo effect in the normal state and therefore we disregard Kondo correlations in the modelling.

To further investigate the importance of multi-level effects, we numerically evaluate the critical current using fourth-order perturbation theory[6,7] (see Supplementary Information for details). We assume that tunnel couplings are random in amplitude and sign (reflecting the parity of wavefunctions) and set $\Delta^*/E_c = 0.1$, as in our experiment. The probability for a negative supercurrent in the centre of a Coulomb diamond, P_π, is plotted in Fig. 4b for odd and even numbers of electrons. A very large average level spacing ($\delta/E_c \gg 1$) effectively gives a single-level quantum dot, so that $P_\pi = 1$ (0) for odd (even) numbers, as explained in Fig. 3a, b. The dependence of the critical current, $I_{c,qd}$, on V_{gate} (Fig. 4c) indeed unambiguously demonstrates the correlation between the number of electrons on the dot and the supercurrent sign. This correlation is absent in the opposite limit ($\delta/E_c \ll 1$), where $P_\pi \approx 0.3$ for both odd and even numbers of electrons, in agreement with previous calculations[7]. From the experimental data in Fig. 1e, we estimate $\delta/E_c \approx 0.4$, which clearly indicates an intermediate regime. Figure 4d shows a typical result for $I_{c,qd}$ versus V_{gate} for $\delta/E_c = 0.4$. As observed in the experiment, we obtain a negative supercurrent for both even (blue dot) and odd (red dot) numbers of electrons. Also, the typical lineshapes closely resemble the experimental data. Thus, in this multi-level regime, co-tunnelling events occur through a single level as well as through different levels. Consequently, the sign of the supercurrent is not only determined by the number of electrons on the quantum dot but also by the wavefunctions of the energy levels.

Received 25 April; accepted 22 June 2006.

1. Josephson, B. D. Possible new effects in superconductive tunnelling. *Phys. Lett.* **1,** 251–253 (1962).
2. Tinkham, M. *Introduction to Superconductivity* 2nd edn (McGraw-Hill, Singapore, 1996).
3. Bulaevskii, L. N., Kuzii, V. V. & Sobyanin, A. A. Superconducting system with weak coupling to the current in the ground state. *JETP Lett.* **25,** 290–294 (1977).
4. Glazman, L. I. & Matveev, K. A. Resonant Josephson current through Kondo impurities in a tunnel barrier. *JETP Lett.* **49,** 659–662 (1989).
5. Spivak, B. I. & Kivelson, S. A. Negative local superfluid densities: The difference between dirty superconductors and dirty Bose liquids. *Phys. Rev. B* **43,** 3740–3743 (1991).
6. Bauernschmitt, R., Siewert, J., Nazarov, Yu. V. & Odintsov, A. A. Josephson effect in low-capacitance superconductor–normal-metal–superconductor systems. *Phys. Rev. B* **49,** 4076–4081 (1994).
7. Rozhkov, A. V., Arovas, D. P. & Guinea, F. Josephson coupling through a quantum dot. *Phys. Rev. B* **64,** 233301 (2001).
8. van Harlingen, D. J. Phase-sensitive tests of the symmetry of the pairing state in the high-temperature superconductors - Evidence for d_{x2-y2} symmetry. *Rev. Mod. Phys.* **67,** 515–535 (1995).
9. Ryazanov, V. V. *et al.* Coupling of two superconductors through a ferromagnet: Evidence for a π-junction. *Phys. Rev. Lett.* **86,** 2427–2430 (2001).
10. Baselmans, J. J. A., Morpurgo, A. F., van Wees, B. J. & Klapwijk, T. M. Reversing the direction of the supercurrent in a controllable Josephson junction. *Nature* **397,** 43–45 (1999).
11. Ralph, D. C., Black, C. T. & Tinkham, M. Spectroscopic measurements of discrete electronic states in single metal particles. *Phys. Rev. Lett.* **74,** 3241–3244 (1995).
12. Black, C. T., Ralph, D. C. & Tinkham, M. Spectroscopy of the superconducting gap in individual nanometer-scale aluminum particles. *Phys. Rev. Lett.* **76,** 688–691 (1996).
13. Buitelaar, M. R., Nussbaumer, T. & Schönenberger, C. Quantum dot in the Kondo regime coupled to superconductors. *Phys. Rev. Lett.* **89,** 256801 (2002).
14. Buitelaar, M. R. *et al.* Multiple Andreev reflections in a carbon nanotube quantum dot. *Phys. Rev. Lett.* **91,** 057005 (2003).
15. Jarillo-Herrero, P., van Dam, J. A. & Kouwenhoven, L. P. Quantum supercurrent transistors in carbon nanotubes. *Nature* **439,** 953–956 (2006).
16. Doh, Y. J. *et al.* Tunable supercurrent through semiconductor nanowires. *Science* **309,** 272–275 (2005).
17. Wagner, R. S. & Ellis, W. C. Vapor-liquid-solid mechanism of single crystal growth. *Appl. Phys. Lett.* **4,** 89–90 (1964).
18. Morales, A. M. & Lieber, C. M. A laser ablation method for the synthesis of crystalline semiconductor nanowires. *Science* **279,** 208–211 (1998).
19. Björk, M. T. *et al.* One-dimensional heterostructures in semiconductor nanowhiskers. *Appl. Phys. Lett.* **80,** 1058–1060 (2002).
20. Verheijen, M. A., Immink, G., de Smet, T., Borgström, M. T. & Bakkers, E. P. A. M. Growth kinetics of heterostructured GaP-GaAs nanowires. *J. Am. Chem. Soc.* **128,** 1353–1359 (2006).
21. Sohn, L. L., Kouwenhoven, L. P. & Schön, G. (eds) *Mesoscopic Electron Transport* (Kluwer, Dordrecht, 1997).
22. Baselmans, J. J. A., Heikkilä, T. T., van Wees, B. J. & Klapwijk, T. M. Direct observation of the transition from the conventional superconducting state to the π state in a controllable Josephson junction. *Phys. Rev. Lett.* **89,** 207002 (2002).
23. Averin, D. V. & Nazarov, Y. V. in *Single Charge Tunneling* (eds Grabert, H. & Devoret, M. H.) Proc. NATO ASI Ser. B 294 217–247 (Plenum, New York, 1991).
24. Björk, M. T. *et al.* Tunable effective g factor in InAs nanowire quantum dots. *Phys. Rev. B* **72,** 201307 (2005).
25. Shimizu, Y., Horii, H., Takane, Y. & Isawa, Y. Multilevel effect on the Josephson current through a quantum dot. *J. Phys. Soc. Jpn* **67,** 1525–1528 (1998).
26. Goldhaber-Gordon, D. *et al.* Kondo effect in a single-electron transistor. *Nature* **391,** 156–159 (1998).
27. Cronenwett, S. M., Oosterkamp, T. H. & Kouwenhoven, L. P. A tunable Kondo effect in quantum dots. *Science* **281,** 540–544 (1998).
28. Choi, M. S., Lee, M., Kang, K. & Belzig, W. Kondo effect and Josephson current through a quantum dot between two superconductors. *Phys. Rev. B* **70,** 020502 (2004).
29. Siano, F. & Egger, R. Josephson current through a nanoscale magnetic quantum dot. *Phys. Rev. Lett.* **93,** 047002 (2004).

Supplementary Information is linked to the online version of the paper at www.nature.com/nature.

Acknowledgements We thank Y.-J. Doh and L. Glazman for discussions, G. Immink for nanowire growth, and A. van der Enden and R. Schouten for technical support. Financial support was obtained from the Dutch Foundation for Fundamental Research on Matter (FOM), the Dutch Organisation for Scientific Research (NWO), the EU programmes HYSWITCH and NODE, and the Japanese International Cooperative Research Project (ICORP).

Author Contributions J.A.v.D., S.D.F. and L.P.K. are responsible for quantum transport experiments, Y.V.N. for numerical simulations, and E.P.A.M.B. for nanowire growth.

Author Information Reprints and permissions information is available at npg.nature.com/reprintsandpermissions. The authors declare no competing financial interests. Correspondence and requests for materials should be addressed to L.P.K. (L.P.Kouwenhoven@TUDelft.nl).